**International Journal of Automobile Engineering Research and Development (IJAuERD)**
**ISSN(P): 2277-4785; ISSN(E): 2278-9413**
**Vol. 4, Issue 1, Feb 2014, 41-54**


# ANALYSIS OF PERFORMANCE OF VARIOUS METAL CATALYSTS USED IN CATALYTIC CONVERTERS WITH MC-2 CONFIGURATION BY C.F.D. TECHNIQUES

**K. S. UMESH[1], V. K. PRAVIN[2] & K. RAJAGOPAL[3]**

[1]Department of Mechanical Engineering, Thadomal Shahani Engineering College, Mumbai, Maharashtra, India

[2]Department of Mechanical Engineering, P.D.A. College of Engineering, Gulbarga, Karnataka, India

[3]Former Vice Chancellor, JNT University, Hyderabad, Andhra Pradesh, India

## ABSTRACT

Catalytic converters are generally fitted in series with the exhaust pipe of almost all vehicles. These Catalytic converters helps in infiltration of harmful pollutants like hydrocarbons (HC), carbon monoxide (CO) and nitrogen oxides (NOx) from the exhaust gases released into atmosphere. They oxidize carbon monoxide (CO) to carbon dioxide (CO2), and reduce nitrogen oxides (NOx) into nitrogen and water vapors. Catalytic converters have become integral part of exhaust system of automobile ever since their first introduction in 1974. More than 96 percent of cars manufactured today are equipped with catalytic converters. Most of the catalytic converters use platinum, Palladium & Rhodium as catalyst to bring about oxidation costly and rarely available. The scarcity and high demand of present catalyst materials necessitate the need for finding out the alternatives. Catalytic converters are available in various designs. Among all other particulate filter materials, knitted steel wire mesh material is selected as filter materials in this paper. In our attempt to analyze filtration performance of catalytic converters working with alternative catalysts for the catalysis, we have chosen copper and Nickel as alternative catalysts for Platinum-Palladium due to similarity in their catalytic properties. Amongst various constituents of exhaust gas, CO and NO are most dangerous pollutants from Global warming point of view. Thus this particular work is concentrated on analyzing filtration efficiency for these two pollutants.

**KEYWORDS:** CFX, CATIA V5, Gambit 2.2, DETCHEM, Fluent 6.2, MC-2 Configuration, Porosity, Wash Coat Thickness, Relative A: F Ratio

## INTRODUCTION

Conversion efficiency of a catalytic converter depends on various factors. It primarily depends upon properties of catalytic converters such as cross section, length, cell density, wall thickness, wash coat and coating. On the other hand the flow characteristics of the exhaust gas such as flow velocity, temperature, composition of raw emissions and flow distribution also influence the conversion efficiency of the catalytic converters.

Large amount of work has already taken place in this field. Andreassi et al. (Muthaiah et al., 2010) investigated about the role of channel cross-section shape on mass and heat transfer processes. The development of catalytic converter systems for automotive applications is, to a great extent, related to monolith catalyst support materials and design. They also studied improvements of converter channels fluid-dynamics aiming to enhance pollutant conversion in all the engine operating conditions. Rajadurai et al. (Kamble and Ingle, 2008) studied the effect of Knitted wire mesh substrates with different geometry and channels on the back pressure of catalytic converter. They considered primary requirements of exhaust after treatment systems of low back pressure, low system weight, better emission performance and lower cost. Combinations of these properties provide better engine performance and higher system value. Ekstrom and Andersson (Beardsley et al.1999) analyzed about the pressure drop behavior of catalytic converter for a number of different substrates,

suitable for high performance IC-engines, regarding cell density, wall thickness and coating. The data has been used to develop an empirical model for pressure drop in catalytic converters. An investigation has been carried out for reducing pollutants from a variable compression ratio, copper-coated spark ignition engine fitted with catalytic converter containing sponge iron catalyst run with gasohol by Narsimha et al. (Eberhard et al., 2005). Mohiuddin and Nurhafez (Jacobs et al., 2006) conducted an experiment to study the performance and conversion efficiencies of ceramic monolith three-way catalytic converters (TWCC) employed in automotive exhaust lines for the reduction of gasoline emissions. Muthaiah et al. (Lahousse et al., 2006) conducted an experimental test on a 10 hp, twin-cylinder, and four-stroke, direct injection and vertical diesel engine. At present, the wall flow ceramic substrate is used as filters which are expensive and also offer more back pressure resulting in more fuel consumption. Kulal et.al (2012) analyzed three different configurations of catalytic converters viz. MC-1, MC-2 and MC-3 for flow characters like velocity distribution & pressure drop to optimize the design for minimum particulate matter in the exhaust.

This paper deals with the study of fluid flow inside the catalytic converter and the study of temperature distribution and chemical reaction in catalytic converter. CATIA V5R-15 was used for geometric modeling of catalytic converter. Domain Discretisation was carried out in Gambit 2.2. Fluent 6.2 was used for carrying out analysis. Flow field in the catalytic converter is influenced by the flow resistance of the substrate for a given geometric configuration. As the mass flow rate increases, the pressure drop also increases. At lower temperature, the catalytic converter will be inactive. The heat release due to chemical reaction at lower temperature does not play a significant role.

The program $DETCHEM_{CHANNEL}$ is used to solve the laminar time-independent boundary-layer equations of a fluid flow through a cylindrical channel. In comparison to the Navier-Stokes equations, the diffusion terms along the direction of convection are neglected. This model has been proven useful for higher flow velocities, as they are expected in this application. In case of a turbulent flow entering the single channel, the parabolic laminar flow profile will quickly be established due to the small channel diameter and low Reynolds number. This entrance effect is modeled by applying a uniform velocity profile at the entrance. If the physical conditions lead to a fully developed turbulent flow enhancing mixing, a plug-flow model may be used as turbulent model.

We have considered two chemical reactions. The oxidation reaction of CO and hydrocarbons and reduction reaction of NO were considered. The hydrocarbons were represented by propylene, which is easily oxidized hydrocarbon, constitute about 80% of the total hydrocarbons found in the typical exhaust gas. The chemical reactions are:

- Oxidation of carbon monoxide

$$2CO+O_2 \rightarrow 2CO_2 \quad (1)$$

- Oxidation of Hydro carbon

$$2C_3H_6+9O_2 \rightarrow 3CO_2+6H_2O \quad (2)$$

- Reduction of Nitrous Oxide

$$CO+NO \rightarrow C02 + ½\ N2 \quad (3)$$

The results obtained have been presented in tabular manner in order to make it easier to compare the models considered for the work.

## MODEL DESCRIPTION

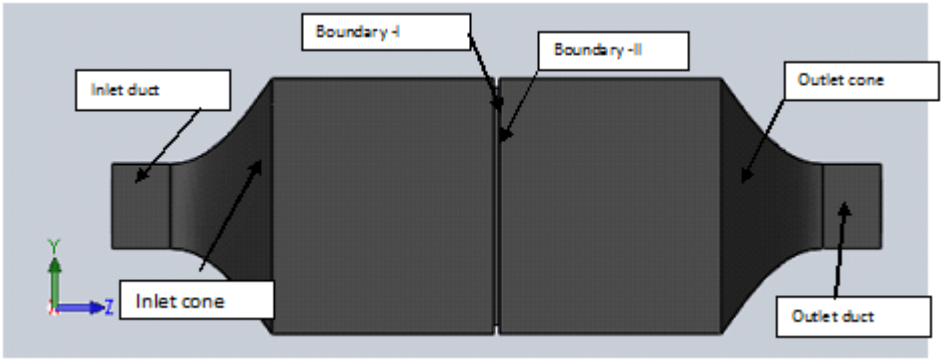


**Figure 1: Catalytic Converter**

For the simulations a commercially available three-way catalytic converter with a rectangular cross-section was assumed. The specifications of the substrate, the coating and the canning are listed in following tables:

**Table 1: Model Description**

| Property | 1St Compartment | 2nd Compartment |
|---|---|---|
| Cell Density (Cells/ Inch$^2$) | 144 | 324 |
| Hydraulic Diameter (mm) | 0.51 | 0.41 |
| Uncoated Wall Thickness (mm) | 8 | 6 |
| Wash coat Thickness (µm) | 20 | 20 |
| Porosity (%) | 57.7 | 50.8 |

**Table 2: Models Considered for the Study**

| Model: 1 | Model: 2 | Model: 3 |
|---|---|---|
| Substrate: Knitted Steel Wire | Substrate: Knitted Steel Wire | Substrate: Knitted Steel Wire |
| Coating: Copper (50gm/ft$^3$) | Coating: Nickel (50gm/ft$^3$) | Coating: Pt/Pd (50gm/ft$^3$) |
| Inlet Dimensions: 38 X 56 mm | Inlet Dimensions: 38 X 56 mm | Inlet Dimensions: 38 X 56 mm |
| Cross Section : 176 X 110 mm | Cross Section : 176 X 110 mm | Cross Section : 176 X 110 mm |
| Length of one Section: 153 mm | Length of one Section: 153 mm | Length of one Section: 153 mm |

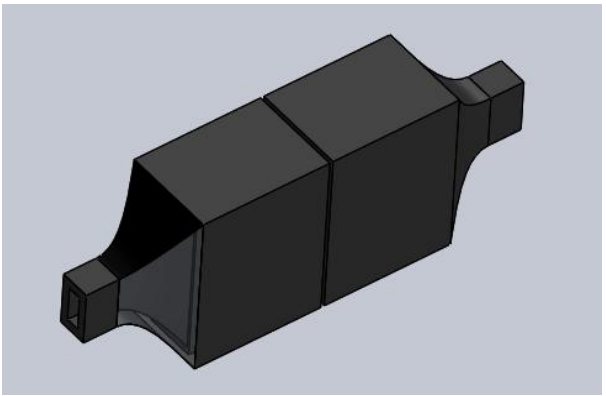

**Figure 2: 3-D view of Catalytic Converter**

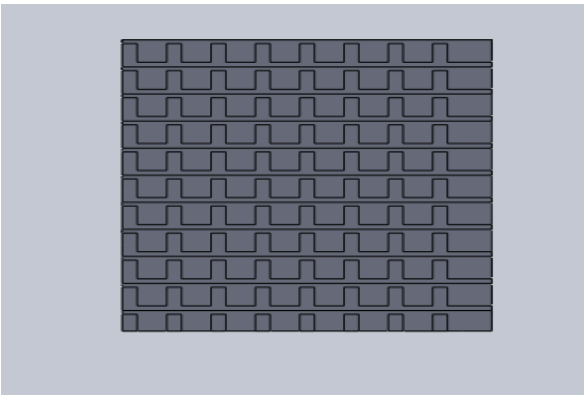

**Figure 3: Side View of Grid**

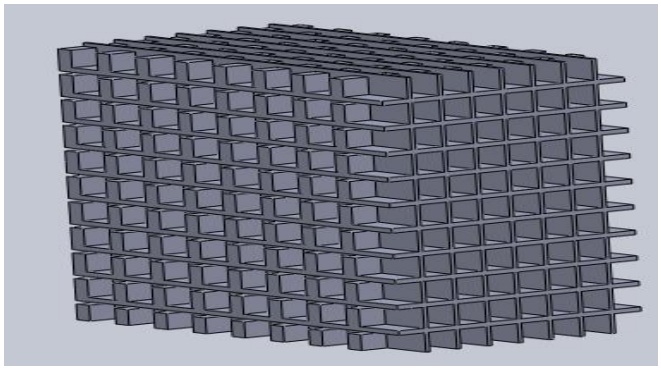

**Figure 4: 3-D View of Grid**

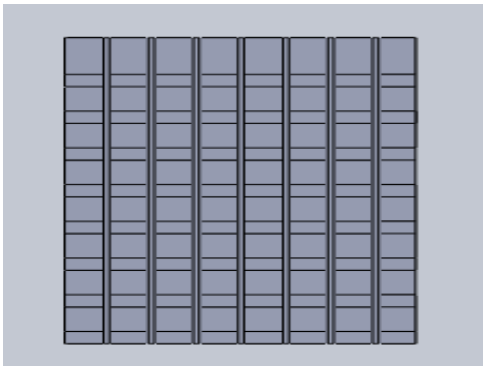

**Figure 5: Top View of Grid**

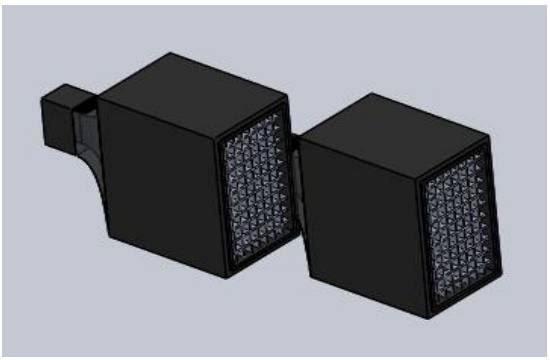

**Figure 6: 3-D View of Two Compartments**

**Figure 7: Assembled Compartment**

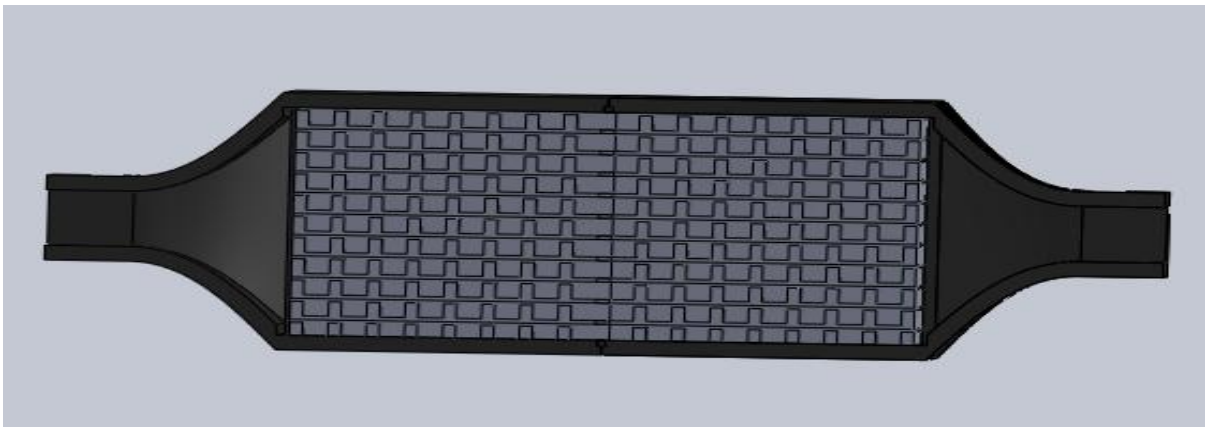

**Figure 8: Path of Exhaust Gas through Catalytic Converter**

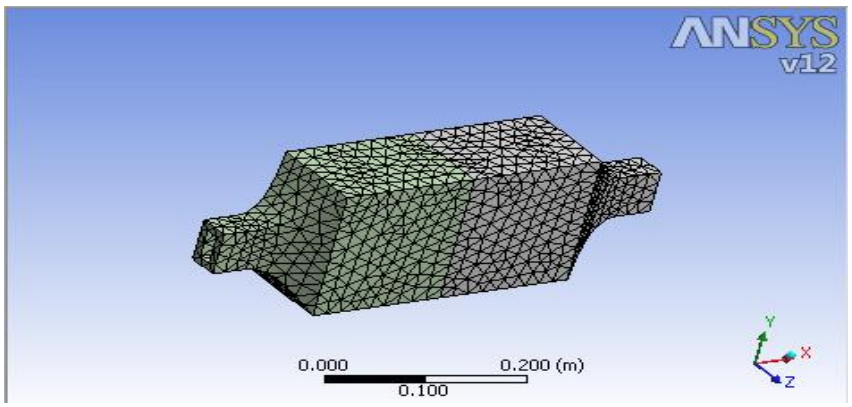


**Figure 9: Meshed Model**

## MATHEMATICAL AND NUMERICAL MODEL

The numerical model for the simulation of the catalytic converter is based on the same assumptions as described before i.e., the time scale of the reactive flow through single channels of the catalytic converter is regarded to be much faster than the thermal response of the catalytic converters' solid core. Then fluctuations in the temperature can be neglected while calculating the fluid flow through a single channel. Thus, a time independent formulation is used to describe the gaseous flow in order to calculate heat source terms for a transient heat conduction equation for the solid.

The equations to be solved are:

- Conservation of total mass

$$\frac{\partial(r\rho u)}{\partial z}+\frac{\partial(r\rho v)}{\partial r}=0 \tag{1}$$

- Conservation of species mass

$$\frac{\partial(r\rho u Y_i)}{\partial z}+\frac{\partial(r\rho v Y_i)}{\partial r}=-\frac{\partial}{\partial r}(rj_i) \tag{2}$$

- Conservation of axial momentum

$$\frac{\partial(r\rho uu)}{\partial z}+\frac{\partial(r\rho vu)}{\partial r}=-r\frac{\partial p}{\partial z}+\frac{\partial}{\partial r}\left(\mu r\frac{\partial u}{\partial r}\right) \tag{3}$$

- Conservation of enthalpy

$$\frac{\partial(r\rho uh)}{\partial z}+\frac{\partial(r\rho vh)}{\partial r}= ru\frac{\partial p}{\partial z}+\frac{\partial}{\partial r}\left(\lambda r\frac{\partial T}{\partial r}\right)-\frac{\partial}{\partial r}\left(\sum_i rj_i h_i\right) \tag{4}$$

Despite the actual shape of the channels, a cylindrical model is used in order to reduce the numerical complexity. Catalytic reactions at the surface are taken into account in terms of the diffusive mean flux $j_i$ at the gas phase wash coat interface in Equation 2.

$$j_{i,surf}=\eta F_{cat/geo} M_i \dot{s}_i \tag{5}$$

$$\dot{s}_i=\sum_{k=1}^{K_s}\nu_{ik} k_{fk}\prod_{j=1}^{N_g+N_s} c_j^{\nu'_{jk}} \tag{6}$$

$$k_{fk}=A_k T^{\beta_k}\exp\left[\frac{-E_{ak}}{RT}\right] f_k\left(\Theta_1,\ldots,\Theta_{N_s}\right) \tag{7}$$

$$f_k\left(\Theta_1,\ldots,\Theta_{N_s}\right)=\prod_{i=1}^{N_s}\Theta_i^{\mu_{ik}}\exp\left[\frac{\varepsilon_{ik}\Theta_i}{RT}\right] \tag{8}$$

The boundary-layer equations can be solved in a single sweep of integration along the axial direction by a method-of-lines procedure using an adaptive integration step size. The radial derivatives are discretized using a finite-volume method. The resulting differential-algebraic equation system is integrated using the semi-implicit extrapolation solver LIMEX.

Using this steady-state channel model, a transient simulation of the thermal behavior of the entire catalytic converter is performed by $DETCHEM_{MONOLITH}$. The solid's temperature field is described by a three-dimensional conservation equation:

$$\frac{\partial T_{monolith}}{\partial t} = \nabla^2 \left( \frac{\lambda T_{monolith}}{\rho c_p} \right) + \frac{q}{\rho c_p} \tag{9}$$

$$q = -\sigma \cdot 2\pi r \, \lambda \frac{\partial T_{gas}}{\partial r}\bigg|_{surface} \tag{10}$$

## BOUNDARY CONDITIONS

The simulation and analysis was carried out at different exhaust temperatures ranging between 250 degree Celsius & 1000 degree Celsius. Also we considered 3-different A: F ratios:

**Table2: A: F Ratio**

| | |
|---|---|
| Rich Mixture | Relative A:F ratio ($\lambda_{OX}$) 0.5 |
| Nearly Stochiometric Mixture | Relative A:F ratio ($\lambda_{OX}$) 0.9 |
| Lean Mixture | Relative A:F ratio ($\lambda_{OX}$) 1.5 |

**Table3: Applied Boundary Conditions**

| Entity | Zone | Zone type |
|---|---|---|
| Mass Flow Inlet | Boundary | Inlet |
| Pressure Outlet | Boundary | Outlet |
| Boundary 1 | Boundary | Wall-Reduction |
| Boundary 2 | Boundary | Wall-Oxidation |

## RESULTS

The results obtained after the mathematical simulation are listed in following Tables:

**Table 4: Conversion Efficiencies with Ni as Catalyst ($\lambda_{OX}$=0.9)**

| Temperature | EMISSION ($\lambda_{OX}$ =0.9) | | | | | |
|---|---|---|---|---|---|---|
| | Carbon Monoxide(CO) | | | Nitrogen Oxide(NO) | | |
| | Mass Fraction at Inlet | Mass Fraction at Outlet | Conversion Efficiency | Mass Fraction at Inlet | Mass Fraction at Outlet | Conversion Efficiency |
| 250 | 0.0135 | 0.013 | 3.7037037 | 0.0015 | 0.00125 | 16.6666667 |
| 325 | 0.0135 | 0.0118 | 12.5925926 | 0.0015 | 0.0013 | 13.3333333 |
| 400 | 0.0135 | 0.01 | 25.9259259 | 0.0015 | 0.0008 | 46.6666667 |
| 475 | 0.0135 | 0.0054 | 60 | 0.0015 | 0.000745 | 50.3333333 |
| 550 | 0.0135 | 0.00487 | 63.9259259 | 0.0015 | 0.000921 | 38.6 |
| 625 | 0.0135 | 0.00452 | 66.5185185 | 0.0015 | 0.000658 | 56.1333333 |
| 700 | 0.0135 | 0.00444 | 67.1111111 | 0.0015 | 0.000624 | 58.4 |
| 775 | 0.0135 | 0.00438 | 67.5555556 | 0.0015 | 0.00068 | 54.6666667 |
| 850 | 0.0135 | 0.00422 | 68.7407407 | 0.0015 | 0.000811 | 45.9333333 |

**Table 4: Contd**

| | | | | | | |
|---|---|---|---|---|---|---|
| 925 | 0.0135 | 0.00438 | 67.5555556 | 0.0015 | 0.000701 | 53.2666667 |
| 1000 | 0.0135 | 0.00421 | 68.8148148 | 0.0015 | 0.000687 | 54.2 |

**Table 5: Conversion Efficiencies with Cu as Catalyst ($\lambda_{OX}$=0.9)**

| Temperature | EMISSION ($\Lambda_{OX}$ =0.9) | | | | | |
|---|---|---|---|---|---|---|
| | Carbon Monoxide(CO) | | | Nitrogen Oxide(NO) | | |
| | Mass Fraction at Inlet | Mass Fraction at Outlet | Conversion Efficiency | Mass Fraction at Inlet | Mass Fraction at Outlet | Conversion Efficiency |
| 250 | 0.0135 | 0.0128 | 5.1851852 | 0.0015 | 0.001 | 33.3333333 |
| 325 | 0.0135 | 0.0098 | 27.407407 | 0.0015 | 0.00092 | 38.6666667 |
| 400 | 0.0135 | 0.00912 | 32.444444 | 0.0015 | 0.000722 | 51.8666667 |
| 475 | 0.0135 | 0.00721 | 46.592593 | 0.0015 | 0.000698 | 53.4666667 |
| 550 | 0.0135 | 0.00521 | 61.407407 | 0.0015 | 0.000547 | 63.5333333 |
| 625 | 0.0135 | 0.00412 | 69.481481 | 0.0015 | 0.000549 | 63.4 |
| 700 | 0.0135 | 0.00385 | 71.481481 | 0.0015 | 0.000602 | 59.8666667 |
| 775 | 0.0135 | 0.00341 | 74.740741 | 0.0015 | 0.000589 | 60.7333333 |
| 850 | 0.0135 | 0.00322 | 76.148148 | 0.0015 | 0.000658 | 56.1333333 |
| 925 | 0.0135 | 0.00344 | 74.518519 | 0.0015 | 0.000623 | 58.4666667 |
| 1000 | 0.0135 | 0.00319 | 76.37037 | 0.0015 | 0.000621 | 58.6 |

**Table 6: Conversion Efficiencies with Pt/Pd as Catalyst ($\lambda_{OX}$ =0.9)**

| Temperature | EMISSION ($\Lambda_{OX}$ =0.9) | | | | | |
|---|---|---|---|---|---|---|
| | Carbon Monoxide(CO) | | | Nitrogen Oxide(NO) | | |
| | Mass Fraction At Inlet | Mass Fraction At Outlet | Conversion Efficiency | Mass Fraction At Inlet | Mass Fraction At Outlet | Conversion Efficiency |
| 250 | 0.0135 | 0.011 | 18.518519 | 0.0015 | 0.00098 | 34.6666667 |
| 325 | 0.0135 | 0.00965 | 28.518519 | 0.0015 | 0.00092 | 38.6666667 |
| 400 | 0.0135 | 0.00898 | 33.481481 | 0.0015 | 0.000699 | 53.4 |
| 475 | 0.0135 | 0.00684 | 49.333333 | 0.0015 | 0.000974 | 35.0666667 |
| 550 | 0.0135 | 0.00547 | 59.481481 | 0.0015 | 0.000512 | 65.8666667 |
| 625 | 0.0135 | 0.00398 | 70.518519 | 0.0015 | 0.000498 | 66.8 |
| 700 | 0.0135 | 0.00341 | 74.740741 | 0.0015 | 0.0005 | 66.6666667 |
| 775 | 0.0135 | 0.00307 | 77.259259 | 0.0015 | 0.00055 | 63.3333333 |
| 850 | 0.0135 | 0.00238 | 82.37037 | 0.0015 | 0.0006 | 60 |
| 925 | 0.0135 | 0.00192 | 85.777778 | 0.0015 | 0.000598 | 60.1333333 |
| 1000 | 0.0135 | 0.00188 | 86.074074 | 0.0015 | 0.000598 | 60.1333333 |

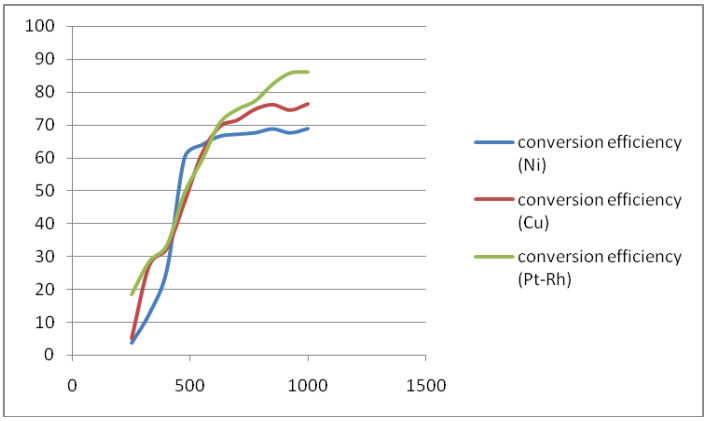


**Figure 10: Conversion Efficiencies (CO) for Different Configurations vs Temperature in Degree Celsius**

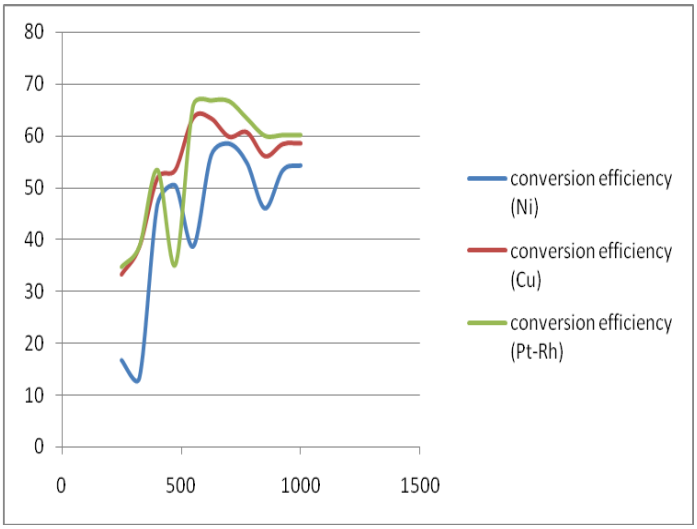


**Figure 11: Conversion Efficiencies (NO) for Different Configurations vs Temperature in Degree Celsius**

**Table 7: Conversion Efficiencies with Ni as Catalyst ($\lambda_{OX}$ =0.5)**

| Temperature | EMISSION ($\Lambda_{ox}$ =0.5) | | | | | |
|---|---|---|---|---|---|---|
| | Carbon Monoxide(CO) | | | Nitrogen Oxide(NO) | | |
| | Mass Fraction at Inlet | Mass Fraction at Outlet | Conversion Efficiency | Mass Fraction at Inlet | Mass Fraction at Outlet | Conversion Efficiency |
| 250 | 0.0135 | 0.0132 | 2.22222222 | 0.0015 | 0.00136 | 9.33333333 |
| 325 | 0.0135 | 0.0113 | 16.2962963 | 0.0015 | 0.001 | 33.3333333 |
| 400 | 0.0135 | 0.00847 | 37.2592593 | 0.0015 | 0.000741 | 50.6 |
| 475 | 0.0135 | 0.00812 | 39.8518519 | 0.0015 | 0.000694 | 53.7333333 |
| 550 | 0.0135 | 0.00715 | 47.037037 | 0.0015 | 0.000542 | 63.8666667 |
| 625 | 0.0135 | 0.00701 | 48.0740741 | 0.0015 | 0.000246 | 83.6 |
| 700 | 0.0135 | 0.00697 | 48.3703704 | 0.0015 | 0.000221 | 85.2666667 |
| 775 | 0.0135 | 0.00651 | 51.7777778 | 0.0015 | 0.000164 | 89.0666667 |
| 850 | 0.0135 | 0.00628 | 53.4814815 | 0.0015 | 0.0002 | 86.6666667 |
| 925 | 0.0135 | 0.00594 | 56 | 0.0015 | 0.000191 | 87.2666667 |
| 1000 | 0.0135 | 0.00503 | 62.7407407 | 0.0015 | 0.000187 | 87.5333333 |

**Table 8: Conversion Efficiencies with Cu as Catalyst ($\lambda_{OX}$ =0.5)**

| Temperature | EMISSION ($\Lambda_{ox}$ =0.5) | | | | | |
|---|---|---|---|---|---|---|
| | Carbon Monoxide(CO) | | | Nitrogen Oxide(NO) | | |
| | Mass Fraction at Inlet | Mass Fraction at Outlet | Conversion Efficiency | Mass Fraction at Inlet | Mass Fraction at Outlet | Conversion Efficiency |
| 250 | 0.0135 | 0.0128 | 5.1851852 | 0.0015 | 0.001 | 33.3333333 |
| 325 | 0.0135 | 0.00993 | 26.444444 | 0.0015 | 0.001 | 33.3333333 |
| 400 | 0.0135 | 0.00721 | 46.592593 | 0.0015 | 0.000589 | 60.7333333 |
| 475 | 0.0135 | 0.00714 | 47.111111 | 0.0015 | 0.000501 | 66.6 |
| 550 | 0.0135 | 0.00602 | 55.407407 | 0.0015 | 0.000395 | 73.6666667 |
| 625 | 0.0135 | 0.00598 | 55.703704 | 0.0015 | 0.000358 | 76.1333333 |
| 700 | 0.0135 | 0.00549 | 59.333333 | 0.0015 | 0.000326 | 78.2666667 |
| 775 | 0.0135 | 0.00584 | 56.740741 | 0.0015 | 0.000186 | 87.6 |
| 850 | 0.0135 | 0.00549 | 59.333333 | 0.0015 | 0.000201 | 86.6 |
| 925 | 0.0135 | 0.00523 | 61.259259 | 0.0015 | 0.000126 | 91.6 |
| 1000 | 0.0135 | 0.00504 | 62.666667 | 0.0015 | 0.000126 | 91.6 |

**Table 9: Conversion Efficiencies with Pt-Pd as Catalyst ($\lambda_{OX}$ =0.5)**

| Temperature | EMISSION ($\lambda_{OX}$ =0.5) | | | | | |
|---|---|---|---|---|---|---|
| | Carbon Monoxide(CO) | | | Nitrogen Oxide(NO) | | |
| | Mass Fraction at Inlet | Mass Fraction at Outlet | Conversion Efficiency | Mass Fraction at Inlet | Mass Fraction at Outlet | Conversion Efficiency |
| 250 | 0.0135 | 0.0135 | 0 | 0.0015 | 0.00098 | 34.6666667 |
| 325 | 0.0135 | 0.00984 | 27.111111 | 0.0015 | 0.00098 | 34.6666667 |
| 400 | 0.0135 | 0.00698 | 48.296296 | 0.0015 | 0.000547 | 63.5333333 |
| 475 | 0.0135 | 0.00694 | 48.592593 | 0.0015 | 0.000487 | 67.5333333 |
| 550 | 0.0135 | 0.00597 | 55.777778 | 0.0015 | 0.000396 | 73.6 |
| 625 | 0.0135 | 0.00542 | 59.851852 | 0.0015 | 0.000314 | 79.0666667 |
| 700 | 0.0135 | 0.00497 | 63.185185 | 0.0015 | 0.000212 | 85.8666667 |
| 775 | 0.0135 | 0.0051 | 62.222222 | 0.0015 | 0.000184 | 87.7333333 |
| 850 | 0.0135 | 0.00498 | 63.111111 | 0.0015 | 0.000182 | 87.8666667 |
| 925 | 0.0135 | 0.00487 | 63.925926 | 0.0015 | 0.000128 | 91.4666667 |
| 1000 | 0.0135 | 0.00476 | 64.740741 | 0.0015 | 0.000122 | 91.8666667 |

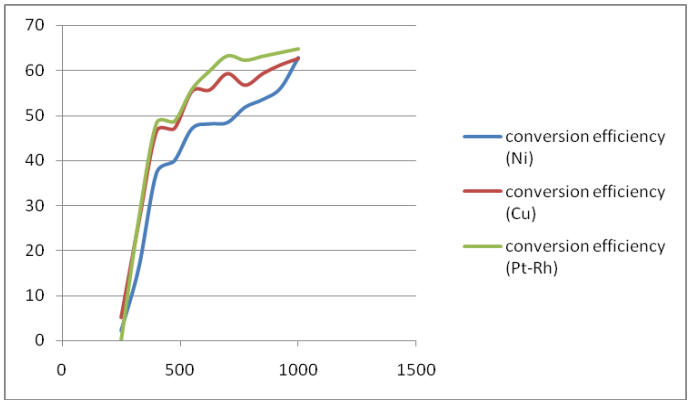


**Figure 12: Conversion Efficiencies (CO) for Different Configurations vs Temperature in Degree Celsius**

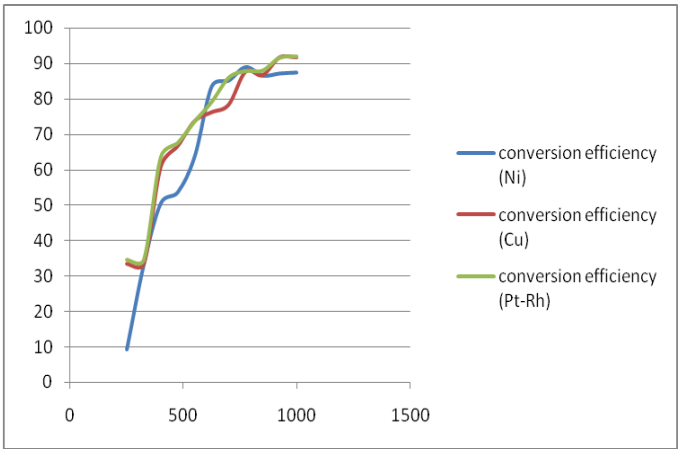


**Figure 13: Conversion Efficiencies (NO) for Different Configurations vs Temperature in Degree Celsius**

**Table 10: Conversion Efficiencies with Ni as Catalyst ($\lambda_{OX}$ =1.5)**

| Temperature | EMISSION ($\Lambda_{ox}$ =1.5) | | | | | |
|---|---|---|---|---|---|---|
| | Carbon Monoxide(CO) | | | Nitrogen Oxide(NO) | | |
| | Mass Fraction at Inlet | Mass Fraction at Outlet | Conversion Efficiency | Mass Fraction at Inlet | Mass Fraction at Outlet | Conversion Efficiency |
| 250 | 0.0135 | 0.013 | 3.7037037 | 0.0015 | 0.001 | 33.3333333 |
| 325 | 0.0135 | 0.00984 | 27.1111111 | 0.0015 | 0.00077 | 48.6666667 |

| Table 10: Contd | | | | | | |
|---|---|---|---|---|---|---|
| 400 | 0.0135 | 0.00751 | 44.3703704 | 0.0015 | 0.00068 | 54.6666667 |
| 475 | 0.0135 | 0.00394 | 70.8148148 | 0.0015 | 0.00067 | 55.3333333 |
| 550 | 0.0135 | 0.00375 | 72.2222222 | 0.0015 | 0.00063 | 58 |
| 625 | 0.0135 | 0.00351 | 74 | 0.0015 | 0.00061 | 59.3333333 |
| 700 | 0.0135 | 0.00356 | 73.6296296 | 0.0015 | 0.00059 | 60.6666667 |
| 775 | 0.0135 | 0.00303 | 77.5555556 | 0.0015 | 0.000574 | 61.7333333 |
| 850 | 0.0135 | 0.00254 | 81.1851852 | 0.0015 | 0.000555 | 63 |
| 925 | 0.0135 | 0.00249 | 81.5555556 | 0.0015 | 0.000532 | 64.5333333 |
| 1000 | 0.0135 | 0.00198 | 85.3333333 | 0.0015 | 0.000517 | 65.5333333 |

**Table 11: Conversion Efficiencies with Cu as Catalyst ($\lambda_{OX}$ =1.5)**

| Temperature | EMISSION ($\Lambda_{ox}$ =1.5) | | | | | |
|---|---|---|---|---|---|---|
| | Carbon Monoxide(CO) | | | Nitrogen Oxide(NO) | | |
| | Mass Fraction at Inlet | Mass Fraction at Outlet | Conversion Efficiency | Mass Fraction at Inlet | Mass Fraction at Outlet | Conversion Efficiency |
| 250 | 0.0135 | 0.0128 | 5.1851852 | 0.0015 | 0.001 | 33.3333333 |
| 325 | 0.0135 | 0.00976 | 27.703704 | 0.0015 | 0.000698 | 53.4666667 |
| 400 | 0.0135 | 0.00802 | 40.592593 | 0.0015 | 0.000621 | 58.6 |
| 475 | 0.0135 | 0.00403 | 70.148148 | 0.0015 | 0.000489 | 67.4 |
| 550 | 0.0135 | 0.00395 | 70.740741 | 0.0015 | 0.000486 | 67.6 |
| 625 | 0.0135 | 0.00371 | 72.518519 | 0.0015 | 0.000654 | 56.4 |
| 700 | 0.0135 | 0.00298 | 77.925926 | 0.0015 | 0.000628 | 58.1333333 |
| 775 | 0.0135 | 0.00224 | 83.407407 | 0.0015 | 0.00058 | 61.3333333 |
| 850 | 0.0135 | 0.00192 | 85.777778 | 0.0015 | 0.000721 | 51.9333333 |
| 925 | 0.0135 | 0.00189 | 86 | 0.0015 | 0.000584 | 61.0666667 |
| 1000 | 0.0135 | 0.00177 | 86.888889 | 0.0015 | 0.000571 | 61.9333333 |

**Table 12: Conversion Efficiencies with Pt-Pd as Catalyst ($\lambda_{OX}$ =1.5)**

| Temperature | EMISSION ($\lambda_{OX}$ =1.5) | | | | | |
|---|---|---|---|---|---|---|
| | Carbon Monoxide(CO) | | | Nitrogen Oxide(NO) | | |
| | Mass Fraction at Inlet | Mass Fraction at Outlet | Conversion Efficiency | Mass Fraction at Inlet | Mass Fraction at Outlet | Conversion Efficiency |
| 250 | 0.0135 | 0.01 | 25.925926 | 0.0015 | 0.000982 | 34.5333333 |
| 325 | 0.0135 | 0.00941 | 30.296296 | 0.0015 | 0.000687 | 54.2 |
| 400 | 0.0135 | 0.00754 | 44.148148 | 0.0015 | 0.000598 | 60.1333333 |
| 475 | 0.0135 | 0.00421 | 68.814815 | 0.0015 | 0.000487 | 67.5333333 |
| 550 | 0.0135 | 0.00368 | 72.740741 | 0.0015 | 0.000454 | 69.7333333 |
| 625 | 0.0135 | 0.00355 | 73.703704 | 0.0015 | 0.0005 | 66.6666667 |
| 700 | 0.0135 | 0.00254 | 81.185185 | 0.0015 | 0.000498 | 66.8 |
| 775 | 0.0135 | 0.00198 | 85.333333 | 0.0015 | 0.000498 | 66.8 |
| 850 | 0.0135 | 0.00159 | 88.222222 | 0.0015 | 0.000496 | 66.9333333 |
| 925 | 0.0135 | 0.00154 | 88.592593 | 0.0015 | 0.000494 | 67.0666667 |
| 1000 | 0.0135 | 0.00152 | 88.740741 | 0.0015 | 0.000487 | 67.5333333 |

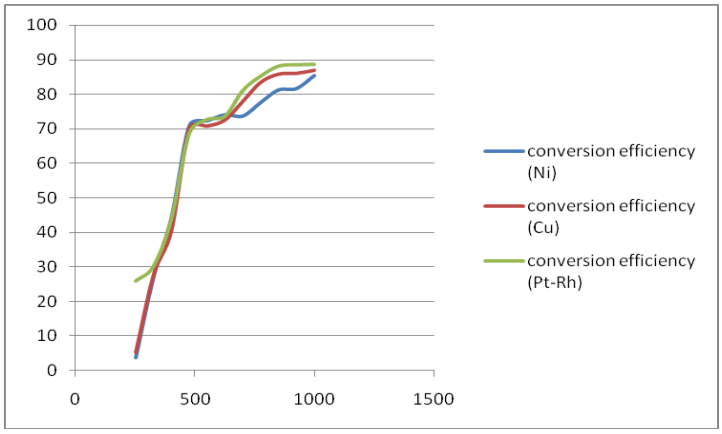


**Figure 14: Conversion Efficiencies (CO) for Different Configurations vs Temperature in Degree Celsius**

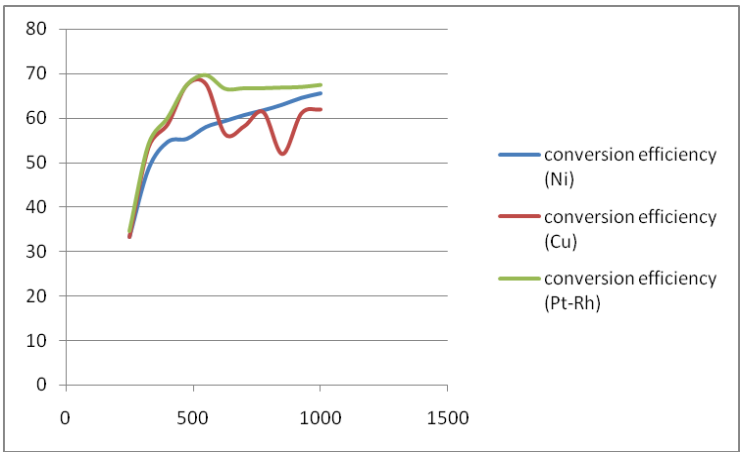


**Figure 15: Conversion Efficiencies (NO) for Different Configurations vs Temperature in Degree Celsius**

## CONCLUSIONS

- The conversion efficiency of catalytic converter using Cu as catalyst is lesser than catalytic converter with Pt/Pd as catalyst but higher than catalytic converter using Ni as catalyst.
- Usually conversion efficiency is higher for $NO_x$ when A: F ratio is rich
- Usually conversion efficiency is higher for CO when A: F ratio is lean
- Form all the plots it can be concluded that activation temperatures for Cu, Ni, & Pt/Pd as a catalyst are around 380,410 & 350 degree Celsius approximately. Thus copper can serve as better alternative catalyst than Nickel due to lower activation temperature & better conversion efficiency over range of exhaust temperature.

## REFERENCES

1. PL.S. Muthaiah, Dr. M. Senthil Kumar, Dr. S. Sendilvelan "CFD Analysis of catalytic converter to reduce particulate matter and achieve limited back pressure in diesel engine" Global journal of researches in engineering – A: Classification(FOR) 091304,091399, Vol.10 Issue 5 (Ver1.0) October 2010.
2. P.R.Kamble and S.S. Ingle "Copper Plate Catalytic Converter: An Emission Control Technique" SAE Number 2008-28-0104.
3. M.B. Beardsley et al., (1999). "Thermal Barrier Coatings for Low Emission", High Efficiency Diesel Engine Applications" SAE Technical Paper 1999-01-2255.

4. Eberhard Jacob, Rheinhard Lammermann, Andreas Pappenherimer, and Diether Rothe "Exhaust Gas After treatment System for Euro 4" Heavy Duty Engines – MTZ 6/2005.

5. Jacobs, T., Chatterjee, S., Conway, R., Walker, A., Kramer, J. And Mueller- Haas, K. "Development of a Partial Filter Technology for Hdd Retrofit" Sae Technical Paper 2006-01-0213.

6. C. Lahousse, B. Kern, H. Hadrane and L. Faillon " Backpressure Characteristics of Modern Three-way Catalysts, Benefit on Engine Performance" SAE Paper No. 2006-01-1062, 2006 SAE World Congress, Detroit, Michigan , April 3-6,

7. 2006.Zbigniew Zmudka, Adam Ciesiolkiewicz "Comprehensive approach to the work of Catalysts in Engine exhaust system", Journal of KONES I.C. Engine, Vol. 11, pp. 368-375

8. A. K. M. Mohiuddin and Muhammad Nurhafez "Experimental analysis and comparison of performance characteristics of catalytic converters including simulation" International Journal of Mechanical and Materials Engineering (IJMME), Vol. 2 (2007), No. 1, 1-7

9. He, L.; Yu, X.-M.; Li, G.-L.; Xu, N. 2012. Dynamic Response of a Three-Way Catalytic Converter, Energy Procedia, Volume 17 Part A, pp. 547-554, ISSN 1876-6102.

10. V. K. Pravin, K.S. Umesh, K. Rajagopal, P.H. Veena "Numerical Investigation of Various Models of Catalytic Converters in Diesel Engine to Reduce Particulate Matter and Achieve Limited Back Pressure" International Journal of Fluids Engineering. ISSN 0974-3138 Volume 4, Number 2 (2012), pp. 75-88.

11. K. S. Umesh ,V. K. Pravin, , K. Rajagopal, P. H. Veena "Optimum solution of catalytic converter with filtration efficiency of trap system by developing limited backpressure in diesel engine" International Research Journal of Engineering Science, Technology and Innovation (IRJESTI) Vol. 1(6) pp. 152-160, September 2012

12. Robert H. Perry and Don W. Green "Perry's Chemical Engineering Handbook" ,Seventh edition, Mc Graw Hill International Editions, Chemical Engineering Series, 1997

## NOTATIONS

- ci concentration
- cp specific heat
- fk dependency function
- hi enthalpy of species i
- h enthalpy of the mixture
- p pressure
- q heat source term
- ji diffusive flux including surface flux
- kfk reaction rate
- r radial spatial coordinate
- A face area

- Ak pre-exponential factor
- Eak activation energy
- Fcat/geo ratio of catalytic to geometric surface area
- Ks number of surface reactions
- Mi molar Mass
- Ng number of gas-phase species
- Ns number of surface species
- R gas constant
- T temperature
- $\lambda_{OX}$ Relative A:F ratio
- T time
- u axial velocity
- v radial velocity
- w normal velocity
- w mean normal velocity
- Yi mass fraction of species i
- z axial spatial coordinate
- βk temperature exponent
- εik coverage dependent change of activation energy
- η washcoat effectiveness factor
- λ thermal conductivity
- γ uniformity index
- μ viscosity
- μik coverage dependent change of reaction order
- νik stoichiometric coefficients
- ρ density
- σ channel density
- Θi surface coverage